Conférence Internationale des Energies Renouvelables (CIER'13) Sousse, Tunisie - 2013

Vol.2
ISSN : 2356-5608

Open angle effects on the aerodynamic performances of a flanged Diffuser Augmented Wind Turbine (DAWT)

Rym Chaker[*1], Mouldi Kardous[*2], Fethi Aloui[*3], Sassi Ben Nasrallah[#4]

[*] *Research and Technology Center of Energy (CRTEn) – BorjCedria Technopark, BP. 95, Hammam-Lif 2050, Tunisia*

[1] rym.chaker@gmail.com

[2] mouldi.kardous@crten.rnrt.tn

[3] aloui_fethi@yahoo.fr

[#] *National Engineering School of Monastir*

Avenue Ibn El Jazzar, Monastir5019, Tunisia

[2] Sassi.bennasrallah@enim.rnu.tn

Abstract— **The flanged diffuser is the most used tool for increasing wind power produced by small wind turbines. The open angle is one of the principal geometric parameters that significantly affect the diffuser performances. Results obtained from numerical simulations and experiments show that the ratio between the free stream velocity and the wind velocity recorded in the inlet section of the diffuser (u/U_∞) increases linearly with the open angle. It reaches a maximum and then decreases before becoming nearly constant. The optimum angle was found to be 10° and 12° respectively for an empty diffuser and for a diffuser shrouding a small wind turbine. This observed behavior was explained by the dynamics of two contrarotating vortices generated directly downstream the flange. Indeed, whenever the open angle become larger than the optimum value, the vortex located nearer the exit area, partially covers the diffuser outlet section. It causes the emergence of a recirculation zone at the diffuser inner wall. This phenomenon happens simultaneously with the wind speed slowing down at the diffuser inlet section.**

Keywords— **Flanged Diffuser, Wind energy, Open angle, Simulation, Fluent, Wind tunnel experiment**

I. INTRODUCTION

To diversify their energy resources, many countries are steadily moving towards renewable energy including wind energy. However, wide-spread of wind energy technology remains limited owing to the low wind speed that characterizes many parts of the world. The power produced by a wind turbine is well known to be proportional to the cubic power of the wind velocity approaching the rotor. This means that even a small amount of wind velocity increase leads to a large increase of the wind turbine energy output. Therefore, many research groups have tried to find out new ways to effectively accelerate the wind velocity at the rotor plane. Most of them are about the Diffuser Augmented wind Turbines (DAWT) [1-4].

A diffuser is an empty frustum-shaped structure characterized by an open angle (θ), a small diameter inlet section (Da) and a large diameter output section (Ds). These sections are separated by a distance (L) representing the length of the diffuser [5-8] (Fig.1 and Fig.2).

Fig. 1 Design of the tested diffuser and the small-scale horizontal axis wind turbine.

The open angle is one of the main parameters that control the mechanism of increasing wind velocity at the inlet section of the diffuser. It has been the subject of several experimental and numerical works [7, 9-12]. The optimum open angle value at which the wind speed reaches a maximum, has been founded to be around 4° and 6°for an empty diffuser [9-10] and larger for a DAWT (10° and more) [7, 13, 14]. Abe et al., (2004) and Toshimitsu et al., (2008), found that when a wind turbine is installed inside the diffuser, it resists air flow and limits the flow separation inside the diffuser [7, 14].

It should be noted that these research have involved a relative limited range of open angles. Also lack information regarding the physical process is recorded. Thus deeply investigation could complete prior works and explain why and how the diffuser open angle affects on the wind velocity increase at the inlet section. The adopted approach is based on numerical simulations and experimental measurements.

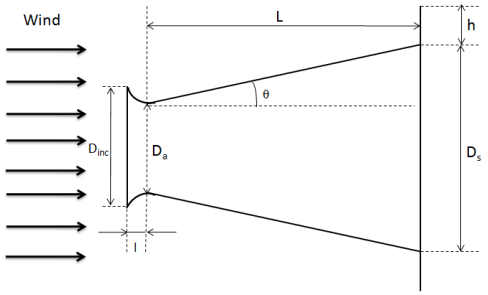

Fig. 2 Geometric characteristics of the tested diffuser.

II. METHODS

In order to investigate the effect of the open angle on the aerodynamic performances of a flanged diffuser, an approach based on numerical simulations and experimental measurements was adopted. Two diffuser configurations were studied. The first one is an empty small-scale diffuser model and the second one is the same diffuser when associated to a small-scale wind turbine (DAWT). However, to analyze the contribution of the diffuser, it was interesting to consider additional configuration of a bare small-scale wind turbine.

The studied flanged diffuser has a curved inlet section. Its length (L), the diameter (Da) of its narrow section and its flange height are fixed. They are 341; 194 and 71 mm respectively. The ratio (L/Da = 1.76) is of the same magnitude as used in previous works [6-8] (Fig.2).

A. CFD Simulations

For both cases (empty diffuser and DAWT), seventeen open angles (θ) ranging from 0° to 35° were tested. The open angles ranged from 0 to 12° are of the same order of magnitude as those used in previous works [9, 10]. Other values (from 14 to 35°) were added to better understanding the flow behavior for larger open angles.

A porous jump condition method was chosen to simulate the small-scale horizontal axis wind turbine that was used in experiments (Fig. 1). It is advisable to remember that the porous jump condition method is a one-dimensional simplification of the porous medium method [15, 16]. It was used successfully for modeling air flow around wind turbines [12, 17].

The thin porous medium has a finite thickness over which a pressure drop occurs. This can be deduced from a combination of Darcy's Law and an additional inertial loss term [15, 18-21] (equation 1).

$$\Delta p = \left(\frac{\mu}{\alpha} v + C \frac{1}{2} \rho v^2 \right) \Delta m$$

μ: The fluid viscosity coefficient (kg.m/s)
α: The permeability of the medium coefficient (m²)
C: The pressure jump coefficient (1/m)
v: The velocity normal to the porous face (m/s)
Δm : The thickness of the medium (m)

However, the use of equation (1), requires to estimate the coefficients α and C first. These can be obtained based on the following hypothesis:

1- Porous media thickness was set to be 2 mm which was thought to be a good approximate value for the thickness of the tested rotor.

2- The term $\left(\frac{\mu}{\alpha} v \right)$ is assumed to be zero [16, 12, 22], consequently, the face permeability of the medium (α) should have a high value. In our case α was set as $1e^{+10}$ m^2.

3- When induction factor (a) is set to 0.19 (this value is obtained in a prior experimented work performed on the small-scale wind turbine S807), then the turbine power coefficient (Cp) and the coefficient C were found to be 0.48 and 234.5/m respectively.

Otherwise, since the flanged diffuser is axisymmetric, two-dimensional simulations (2D) were performed on only the half of the diffuser. The computational domain was constructed using GAMBIT. It was meshed into about 11000 quadrilateral cells using the structured mesh. Cells were gradually condensed toward the diffuser inlet and outlet sections where air flow dynamics is expected to be more active (Fig.3).

At the entrance of the domain (inflow boundary), free stream was initialized at a mean velocity of 5 m.s-1 that gives a Reynolds number of 66500 (by referring to the diffuser inlet section). The other boundary conditions were chosen as follows: atmospheric pressure at the exit section (outflow boundary), a symmetry line for the bottom section and the top section and no-slip boundary condition at the wall of the diffuser (Fig.4).

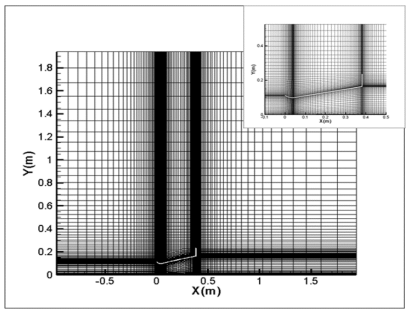

Fig. 3 Computational domain and meshes

Numerical simulations were carried out using FLUENT 6.3 which is a useful computer program for modeling fluid flow in complex geometry. The physics of air flow around and within the diffuser is governed by the incompressible Navier-Stokes equations. A first order discretization scheme was used and a 10-6 residual convergence criterion was chosen.

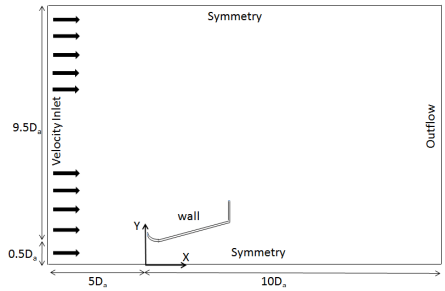

Fig. 4 Boundary conditions

The adopted numerical model is the shear stress transport (SST) K-ω turbulence model. It was developed to effectively blend the robust and accurate formulation of the K-ω model in the near-wall region with the free-stream independence of the K-ε model in the far field [19, 22]. In particular, this model developed by Menter [19] has shown its capability to detect attached and slightly separated flows. Nowadays, it is widely used for wind turbine computation.

To insure that computational conditions do not significantly affect simulations results, three grid systems and three Reynolds number values were tested. Differences between the obtained maximum velocities (at the inlet section of the diffuser) have not exceeded 2% [17]. In consequence, this is reassuring about the quality of the results obtained by the numerical model.

B. Wind Tunnel experiments

Experiments were performed in the wind tunnel of the Research and Technologies Center of Energy Borj Cedria (Tunisia). It is a closed-loop wind tunnel with a total length of 14.6 m and a width of 4.8 m. The test section has 800 mm width, 1000 mm depth and 4000 mm length. The wind velocity inside the wind tunnel can vary from 0 to about 30 m/s. The free stream velocity was measured via a Pitot tube positioned at $10\times D_a$ upstream of the diffuser, While measurements of wind velocity, at several points along the diffusers centerline, were carried out with a second Pitot tube. The accuracy of this device is about 1%. The air temperature variations were considered negligible for the current tests.

III. Results and Discussion

A. Flow description

For the empty diffuser as for the DAWT, two vortices are generated behind the flange producing a low-pressure region. This allows air flow to accelerate inside the narrow inlet section where the maximum of wind velocity (u) was recorded [23] (Fig.5). This result is expected since it was also found hardly in all previous studies including simulations and wind tunnel experiments [7, 8, 10].

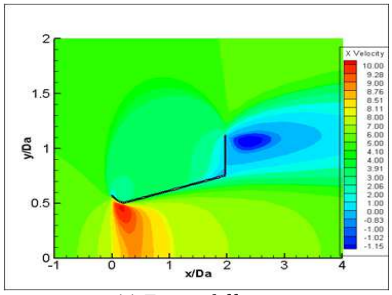

(a):Empty diffuser

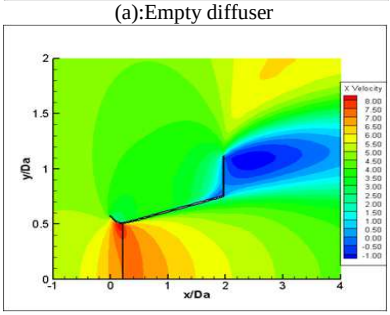

(b): Association diffuser-porous media

Fig. 5 Velocity contours obtained from numerical simulations: (a). Empty diffuser, (b). Association diffuser-porous media.

Figure 6 represents for the three tested configurations, the velocity ratio u/U_∞ versus a dimensionless length x/D_a. The ratio u/U_∞ was considered for the same wind conditions, at a point located at the rotor disk centerline.

As shown by this figure, the ratio (u/U_∞) reaches values of 1.75 and 1.45 respectively for an empty diffuser and a DAWT. Roughly similar experimental results were obtained (1.83 for the empty diffuser and 1.40 for the DAWT). We underline that the ratio u/U_∞ is greater in the case of the empty diffuser than that of the DAWT in both simulations and experiments. The drop in the ratio u/U_∞, while passing from an empty diffuser to a DAWT is calculated equal to 19%. This obviously dues to the resistance effect of the porous disc. From figure 6, wind velocity at the rotor disk is ranged as follows: $u/U_{\infty PourousDisc} < u/U_{\infty DAWT} < u/U_{\infty EmptyDiffuser}$.

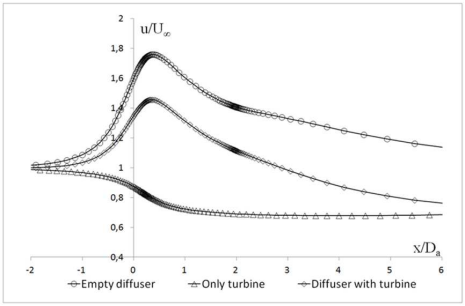

Fig. 6 u/U_∞ vs. x/D_a simulations results (θ=12°)

B. Open Angle Effect

By plotting the wind velocity ratio (u/U_∞) against the open angle (θ) for the empty diffuser and the DAWT, we can see that curves have similar shape (Fig.7).

In both cases, wind velocity ratio (u/U_∞) increases as the opening angle increases. It attains a peak then decreases before becoming nearly constant. The ratio (u/U_∞) reaches a maximum value of 1.76 when θ=10° (for the empty diffuser) and 1.45 when θ=12° (for the DAWT). Thus θ=10° and θ=12° could be suggested as an optimum angles for the empty diffuser and DAWT respectively [24]. It should be noted that u/U_∞ has decreased by 14% for the empty diffuser and only by 3% for the DAWT.

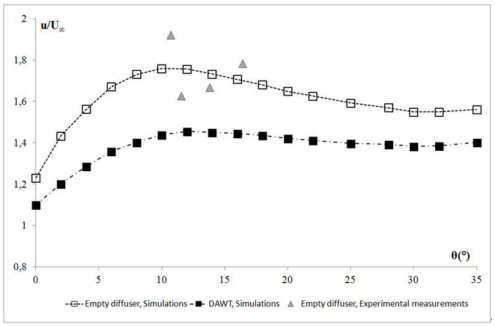

Fig. 7 Velocity ratio u/U_∞ versus open angle.

To better understand this behavior, we have plotted and analyzed the stream lines corresponding to the area located directly downstream the flange for different open angles surrounding the optimal one (Fig.8).

Obtained figure clearly show that just beyond the optimal angle, a recirculation zone emerges at the diffuser inner wall

adjacent to the exit area. That corresponds to the detachment of the boundary layer.

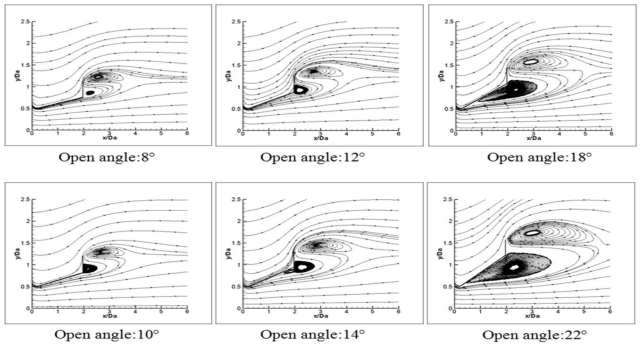

Fig. 8 Stream lines downstream of the empty diffuser for open angles including the optimal one

Above the optimal angle values, boundary layer separation has been grown quickly (Fig.8). For larger angles, this phenomenon has caused a notable disturbance in the air flow, and as mentioned above, it has induced a significant decrease of the wind velocity ratio (u/U_∞) (Fig.7). Nevertheless, when a wind turbine is installed in the diffuser (DAWT), the beginning of the boundary layer separation is rather less severe. That is why the decrease of the wind velocity ratio is less significant and therefore, the optimal open angle of a DAWT is relatively larger than that of an empty diffuser (Fig.7).

C. Open angles and dynamics of contra-rotating vortices

As mentioned in section III.1, streamlines induced by the air flowing around the diffuser show two contra-rotating vortices directly beyond the diffuser flange (Fig. 8). The exact location of theses vortices changes with the open angle value. This dynamic can be characterized based on:

- The (x, y) center coordinates of the vortex 1 and 2: $\mathbf{C_1}$ (x_{C1}, y_{C1}) and $\mathbf{C_2}$ (x_{C2}, y_{C2}) respectively.
- The distance between the two centers **D1**.
- The distance to a reference point $\mathbf{C_{ref}}$ (x_{Cref}, y_{Cref}) located at the intersection between the flange and the exit area of the diffuser (Fig. 9). We note that by conception, the x coordinate of this point is constant while the y coordinate varies according to the diffuser open angle.

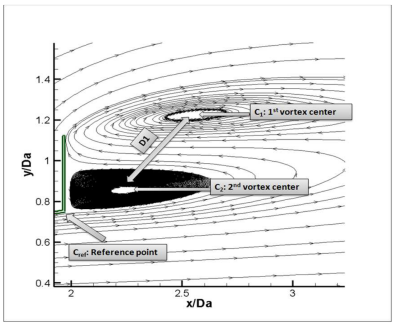

Fig. 9 Distances and centers characterizing vortices downstream the flange

1st vortex dynamic

By plotting the first vortex coordinates (y_{C1} vs. x_{C1}) for the entire tested open angles (θ), we realize that the obtained curves have the same shape for both the empty diffuser and the DAWT (Fig.10). In all cases the 1st vortex center is located above the flange level.

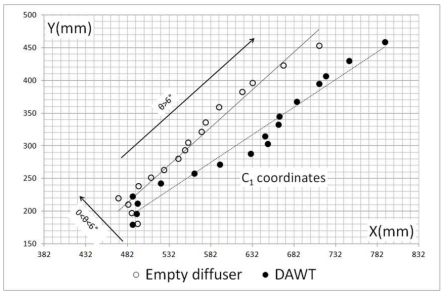

Fig. 10 The 1st vortex center Coordinates

For the open angles included in the interval $0 < \theta \leq 6$, this vortex tends to move toward the flange plane over a short distances. While when θ becomes greater than 6°, it moves away for a relatively longer distance following an ascending straight path. With respect to the flow direction, this straight path has an average angle of about 36° (empty diffuser) and 55° (DAWT). Analyze of data also show that the 1st vortex generated by the DAWT moves twice as fast as the one induced by the empty diffuser. This observation refers only to the vortex motion along x-axis for open angles ranged from 6° to 16°. For other cases, this speed is constant (Fig.11).

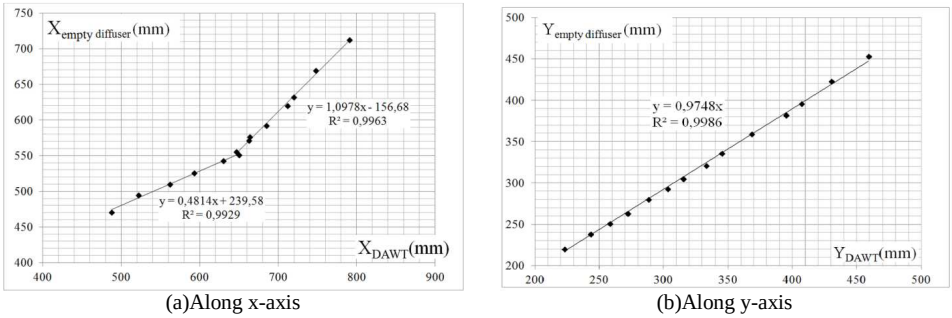

(a)Along x-axis (b)Along y-axis

Fig. 11 The 1st vortex displacement speed

2nd vortex dynamic

The center coordinates of the 2nd vortex for the whole tested open angles (θ) are represented in Figure 12. The obtained curves have similar shape for both configurations empty diffuser and DAWT and are characterized by two segments.

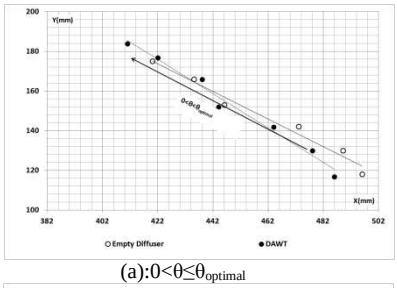

(a):$0<\theta\leq\theta_{optimal}$

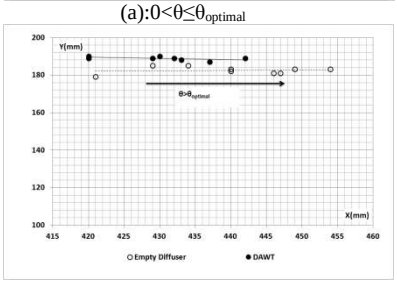

(b):$\theta>\theta_{optimal}$

Fig. 12 The two segment of 2nd vortex center coordinates

At first sight, the 2nd vortex dynamics along the y-axis is fairly limited. However, its effect on the diffuser performances is a determining factor.

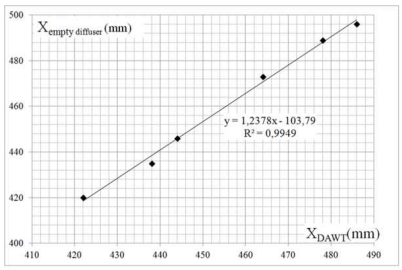

(a): Along x-axis

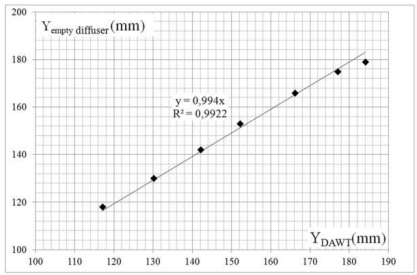

(b): Along y-axis

Fig. 13 The 2nd vortex displacement speed ($0\leq\theta\leq\theta_{optimal}$)

The first segment is a straight line which decreases with the open angle (θ). It concerns angles less than the optimal angle (Fig.12.a). For this range of angles, the motion of the 2nd vortex toward the flange plane is very similar (quantitatively and qualitatively) to that of the 1st vortex. Nevertheless, along the flow direction, the 2nd vortex generated by the empty diffuser approaches the flange a little faster than the one generated by the DAWT (Fig.13.a). In other words, the presence of the turbine causes the 2nd vortex motion along x-axis to slow down. However, the speed remains constant along the y-axis (Fig.13.b).

The second segment (Fig.12.b) is roughly horizontal and located at y =188. It starts when the opening angle becomes greater than the optimal one. For these angles, the 2nd vortex moves away and become farther from the flange as the open angle increases (Fig.12.b).

- The first zone (***Zone 1***) corresponds to angles ranged from 0 to 10° (the empty diffuser) and from 0 to 12° (DAWT). It corresponds to the straight horizontal line of the curve. In this case, the 2nd vortex is substantially stationary along the y-axis and the diffuser reaches its better performances when θ tends towards its optimum value.
- The second zone (***Zone 2***) concerns angles from 10° to 14 ° (the empty diffuser) and from 12° to 15° (DAWT), where the 2nd vortex starts to move downward. When its lower part begins to partially cover the diffuser outlet section, the air flow becomes disturbed and a recirculation zone emerges at the diffuser inner wall adjacent to the outlet section. That corresponds to the boundary layer separation (Fig.8). This phenomenon happens simultaneously with the wind speed slowing down at the diffuser inlet section (Fig.7). At 14° (Empty diffuser) and 15° (DAWT), C_2 is located exactly in horizontal plane passing through the reference point (C_{ref}).
- The third zone (***Zone 3***) concerns open angles greater than 14° (Empty diffuser) and 15° (DAWT). For these angles, C_2 is located downright below the reference point (C_{ref}). Whenever the distance between C_2 and C_{ref} increases, the portion of the diffuser outlet section covered by the vortex become larger, and depending on the diffuser configuration (Empty or including a wind turbine), the effect of swirl on the air flow is more or less intense.

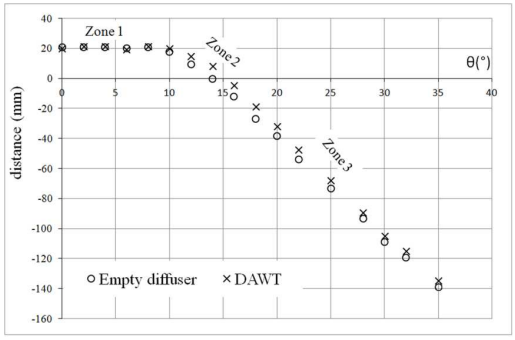

Fig. 14 The distance between C_2 and C_{ref} along y-axis vs. the open angle

<u>The distance between the two vortices centers</u>

By plotting the distance D1 between C_1 and C_2 vs. the open angle (θ) (Fig.15), we found that for low values of θ (0 to 6°), D1 increases slightly and vortices remain close to each other. Beyond θ=6°, both vortices move away from each other as the open angle increases.

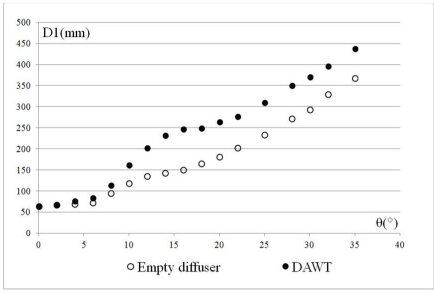

Fig. 15 The variation of the distance between two centers for empty diffuser and DAWT.

For open angles included in the interval $12°<\theta<14°$ (for the empty diffuser) and $14°<\theta<20°$ (for the DAWT), the distance D1 is almost constant, but it is greater in the case of the DAWT than that of the empty diffuser. It should be underlined that these intervals correspond to the situation where the 2nd vortex center goes below the horizontal plane passing through C_{ref} (Fig.15).

IV. CONCLUSIONS

To get a better understanding of the effect of the open angle on wind velocity increase at the inlet section of an empty flanged diffuser and an association diffuser-turbine (DAWT), numerical simulations and wind tunnel experiments have been carried out on seventeen open angle ranged from 0° to 35°. Obtained results show that the wind velocity at the inlet section of the diffuser increases as the open angle increases from 0° to an optimum angle that is 10° for the empty diffuser and 12° for the DAWT. Beyond these optimum angles, the wind velocity decreases before becoming nearly constant. The values of the optimum angles and therefore the wind velocity at inlet section of the diffuser are strongly linked to the dynamics of two contrarotating vortices generated in the region located behind the diffuser. Indeed, whenever the open angle become larger than the optimum value, the vortex located nearer the exit area, partially covers the diffuser outlet section. It causes the air flow to become disturbed and a recirculation zone emerges at the diffuser inner wall (boundary layer separation). This phenomenon happens simultaneously with the wind speed slowing down at the diffuser inlet section.

REFERENCES

[1] G. M. Lilley and W. J. Rainbird, "A Preliminary Report on the Design and Performance of Ducted Windmills, " College of Aeronautics: Cranfield, UK, CoA Rep. , 102, 1956,.

[2] A. Kogan, A. Seginer, "Shrouded Aerogenerator Design Study II, Axisymmetrical shroud performance," in *Proc.5th Annu. Conf. on Aviation and Astronomic*, Tel-Aviv, Israel, (1963).

[3] O. Igra, "Compact shrouds for wind turbines", *Energy Conversion.* Vol.16 pp. 149-157, 1977.

[4] B. L. Gilbert, R. A. Oman and K. M. Foreman, " Fluid dynamics of diffuser-augmented wind turbines," *J. Energ*., Vol. 2:6, pp.368-374, 1978.

[5] M.O.L Hansen, N. N. Sorensen and R. G. J. Flay, " Effect of placing a diffuser around a wind turbine, " *J. Wind. Energy*, Vol.3:4, pp.207-213, 2000.

[6] Y.Ohya and T. Karasudani, "A Shrouded Wind Turbine Generating High Output Power with Wind-lens Technology," *J. Energies*, Vol.3, pp.634–649, 2010.

[7] K. Abe and Y. Ohya, "An investigation of flow fields around flanged diffusers using CFD," *J. Wind Eng. Ind. Aerod.*, Vol.92, pp.315-330, 2004.

[8] Kardous M., Chaker R., Aloui F. and Ben Nasralah S., "On the Dependence of an Empty Flanged Diffuser Performance on Flange Height: Numerical Simulations and PIV Visualizations," *Renew. Energ.*, Vol.56, pp.123-128, 2013.

[9] Y. Ohya, T. Karasudani, A. Sakurai, K. I. Abe and M. Inoue, "Development of a shrouded wind turbine with a flanged diffuser," *J. Wind Eng. Ind. Aerod.*, Vol.96, pp.524-539, 2008.

[10] T. Matsushima, S. Takagi, S. Muroyama, "Characteristics of a highly efficient propeller type small wind turbine with a diffuser," *Renew. Energ*., Vol. 31, pp.1343-1354, 2006.

[11] D.L.F. Gaden, and E.L. Bibeau, "A numerical investigation into the effect of diffusers on the performance of hydro kinetic turbines using a validated momentum source turbine model," *Renew. Energ.*, Vol.35, pp.1152–1158, 2010.

[12] P. Khunthongjan, and A. Janyalertadun, "A study of diffuser angle effect on ducted water current turbine performance using CFD," *Songklanakarin J. Sci. Technol.*, Vol.1:34, pp.61-67, 2012.

[13] K. Abe, M. Nishida, A. Sakurai, Y. Ohya, H. Kihara, E. Wada and, K. Sato, "Experimental and numerical investigations of flow fields behind a small wind turbine with a flanged diffuser," *J. Wind Eng. Ind. Aerod.*, Vol.93, pp.951-970, 2005.

[14] K. Toshimitsu, K. Nishikawa, W. Haruki, S. Oono, M. Takao and Y.Ohya, "PIV Measurements of Flows around the Wind Turbines with a Flanged-Diffuser Shroud," *Int. J. Therm. Sci*., Vol.4:17, pp.375−380, 2008.

[15] Fluent Documentation, 2006.

[16] L. Guo and R. G. Maghirang, "Numerical simulation of airflow and partical collection by vegetative barriers," *Eng. Appl. Comp. Fluid*, Vol.6, pp.110-122, 2012.

[17] Chaker R., Kardous M., Aloui F., and Ben Nasrallah S., "Relationship between open angle and aerodynamic performances of a DAWT," in P*roc. IREC'13*, 20-22 December , 2012, p. 93-100, Sousse.

[18] M. E. Harrison, W. M. J. Batten, L. E. Myers, and A. S. Bahaj, "A comparison between CFD simulations and experiments for predicting the far wake of horizontal axis tidal turbines," in *Proc. the 8th EWTEC*, 2009, p. 566-575, Uppsala, Sweden.

[19] A. T. J. Mozafari, "Numerical Modeling of Tidal Turbines: Methodology Development and Potential Physical Environmental Effects," thesis, University of Washington, 2010.

[20] A.R. Gravdahl, G. Crasto, and F. Castellani, "Wake modeling with the actuator disc concept," in *proc. Deep Wind, Deep sea offshore wind power*, January 2012, p.19-20, Trondheim.

[21] A. El Marjani, F. Castro, M. Bahaji, and B. Filali, "3D unsteady flow simulation in an OWC wave converter plant," in *Proc. Int. Conf. Renew. Ener. and Power Qual. (ICREPQ'06)*, 2006, Mallorca, Espagne.

[22] L. Bai, R. R. G. Spence, and G. Dudziak, "Investigation of the influence of array arrangement and spacing on tidal energy converter (TEC) performance using a 3-Dimensional CFD Model," in *Proc. the 8th Eu. Wave and Tidal Ener.Conf.*, 2009, Uppsala, Sweden.

[23] M. Kardous, R. Chaker, and F. Aloui, "Half-term report of project: Study, design and construction of a augmented wind turbine, " Research and technology center energy Borj Cedria Technopark, p.13-18, 2012.

[24] Ravi Anant Kishore, Thibaud Coudron, Shashank Priya, "Small-scale wind energy portable turbine (SWEPT), " *J. Wind Eng. Ind. Aerod.*, Vol.116, pp.21-31, 2013.